A Further Investigation of NH$_4^+$ Removal Mechanisms by Using Natural and Synthetic Zeolites in Different Concentrations and Temperatures

Huei-Fen Chen [1,2,*], Yi-Jun Lin [1], Bo-Hong Chen [1], Iizuka Yoshiyuki [3], Sofia Ya-Hsuan Liou [4] and Rong-Tan Huang [5]**

[1] Institute of Earth Sciences, National Taiwan Ocean University, Keelung 20224, Taiwan; yijun089@gmail.com (Y.-J.L.); m98860007@mail.ntou.edu.tw (B.-H.C.)
[2] Center of Excellence for Oceans, National Taiwan Ocean University, Keelung 20224, Taiwan
[3] Institute of Earth Sciences, Academia Sinica, Taipei 11529, Taiwan; yiizuka@earth.sinica.edu.tw
[4] Department of Geosciences, National Taiwan University, Taipei 10617, Taiwan; yhliou@ntu.edu.tw
[5] Institute of Materials Engineering National Taiwan Ocean University, Keelung 20224, Taiwan; rthuang@mail.ntou.edu.tw
[*] Correspondence: diopside0412@yahoo.com.tw; Tel.: +886-2-24622192 (ext. 6519)

Abstract: We investigated the ammonium removal abilities of natural and synthetic zeolites with distinct Si/Al ratios and various surface areas to study how adsorption and ion exchange processes in zeolites perform under different ammonium concentrations and different temperatures. Five zeolites—natural mordenite, chabazite, erionite, clinoptilolite, and synthetic merlinoite—were immersed in 20, 50, and 100 mg/kg ammonium solutions. The results demonstrate that zeolites under high ammonium concentrations (100 mg/kg) possess higher physical adsorption capacity (0.398–0.468 meq/g), whereas those under lower ammonium concentrations (20 mg/kg) possess greater ion exchange properties (64–99%). The ion exchange ability of zeolites is extremely dependent on the cation content of the zeolites, and the cation content is affected by the Si/Al ratio. The surface area of zeolites also has a partial influence on its physical adsorption ability. When the surface area is less than 100 m^2/g, the adsorption ability of zeolite increases obviously with surface area; however, adsorption ability is saturated as the surface area becomes larger than this critical value of 100 m^2/g. When we placed the zeolites in 50 mg/kg ammonium concentration at different temperatures (5–50 °C), we found that the zeolites exhibited the highest ammonium removal ability at 30 °C and the potassium release was enhanced at 30–40 °C.

Keywords: zeolite; ion exchange; adsorption; ammonium; Si/Al; temperature

1. Introduction

Natural zeolites are microporous aluminosilicate minerals with high cation exchange capacities and high ammonium selectivity properties [1]. More than 50 different species of this mineral have been identified. Previous researchers have studied the ammonium removal ability of zeolites in the purification of livestock wastewater, landfill wastewater, and aquaculture water [2,3]. In polluted systems, toxic NH$_3$ is transformed to NH$_4^+$ under NH$_4^+$-reducing conditions. Zeolites can effectively remove NH$_4^+$ in water and waste products in order to weaken the virulence of NH$_3$. Natural zeolites, including clinoptilolite [1], mordenite [4], erionite [5], and chabazite [6] have been widely utilized in water purification. Previous studies revealed the mechanisms of NH$_4^+$ removal through ion exchange and adsorption in different zeolites [7,8]. Mordenite and clinoptilolite have frequently been employed to remove ammonium [9]. Many previous investigations have been primarily concerned

with equilibrium isothermal and kinetic models of ammonium adsorption on zeolites at different temperatures, pH, or initial concentrations [10–15]. In this study, we wanted to compare a wider range of Si/Al ratios in zeolites. In order to understand the effect on adsorption and ion exchange capacities, we also measured the cation concentration of the reaction solutions. Moreover, we investigated the concentration and temperature effect on the ion exchange and adsorption mechanism. Cation release ability should be regarded as an important issue that can be advantageously applied in ecosystems and environmental treatments.

2. Materials

Different natural zeolites often grow together or coexist with other minerals; hence, the identification of zeolite composition is imperative. The natural zeolites that were used in this study include chabazites and erionites from Arizona, USA; clinoptilolites acquired from China; and mordenites from Japan. Furthermore, we deliberately synthesized pure merlinoite to manually create a zeolite composition with a lower Si/Al ratio than those of natural zeolites. The synthetic method was designed based on our previous studies by employing glass materials [16,17]. The five samples were identified by X-ray Diffraction (XRD, MAC, Science Mxp 3, Yokohama, Japan) using a Cu target with the Cu Kα wavelength through a 1° divergent slit. Operating conditions were established as 45 kV and 40 mA, the scanning step size was 0.0083556°/s, and a step of 1.27 s was used in the 2θ range of 3°–80°. Mineral identifications by XRD are shown in Figure 1. Most of the zeolites were very pure, and only the chabazite contained a small amount (~5%) of quartz.
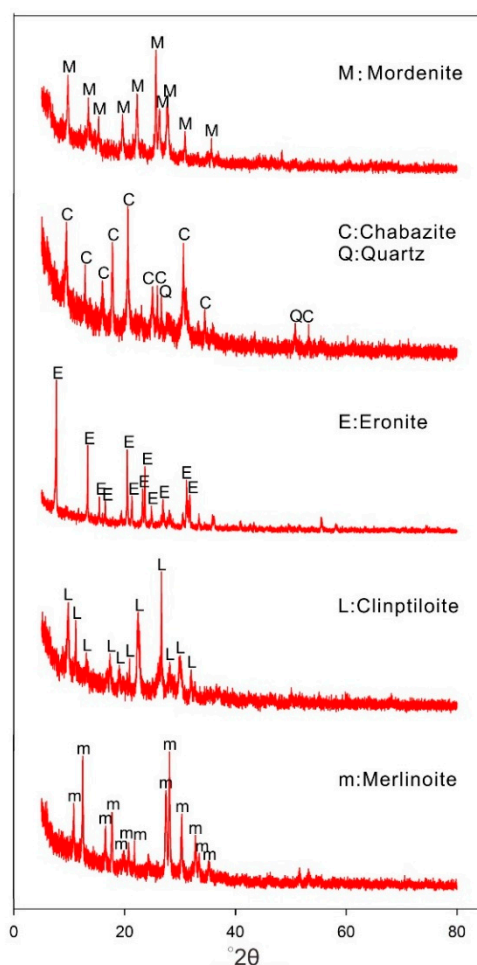

Figure 1. X-ray Diffraction (XRD) results of each zeolite sample.

The morphology of the zeolites (shown in Figure 2) was identified by Scanning Electron Microscopy (SEM, Hitachi, model S-4800, Tokyo, Japan). All of the samples revealed good crystal forms and crystallinity. Chemical analyses were performed by way of Electron Probe Microanalyses (EPMA, JEOL, model JXA-8900 R, Tokyo, Japan) as a method for analyzing each grain of zeolite [18]. The results of the chemical composition analyses of the zeolites are shown in Table 1. Operating conditions were established with an accelerating voltage of 15 kV and the electronic current was set at 5 nA. The two electron beam sizes were less than 5 and 10 μm, and the detection times were set at 10 and 15 s, respectively. Albite and silicate glass were chosen as the chemical standards. Average data for each sample were acquired from more than four individual grains, and each grain was repeatedly tested three times. Table 1 presents the averaged weight percentage of the chemical composition, the Si/Al molar ratios, and the moles of 2Ca + 2Mg + Na + K based on 96 oxygen molecules for each zeolite. The Si/Al ratios of these zeolites range between 2.19 and 5.73.
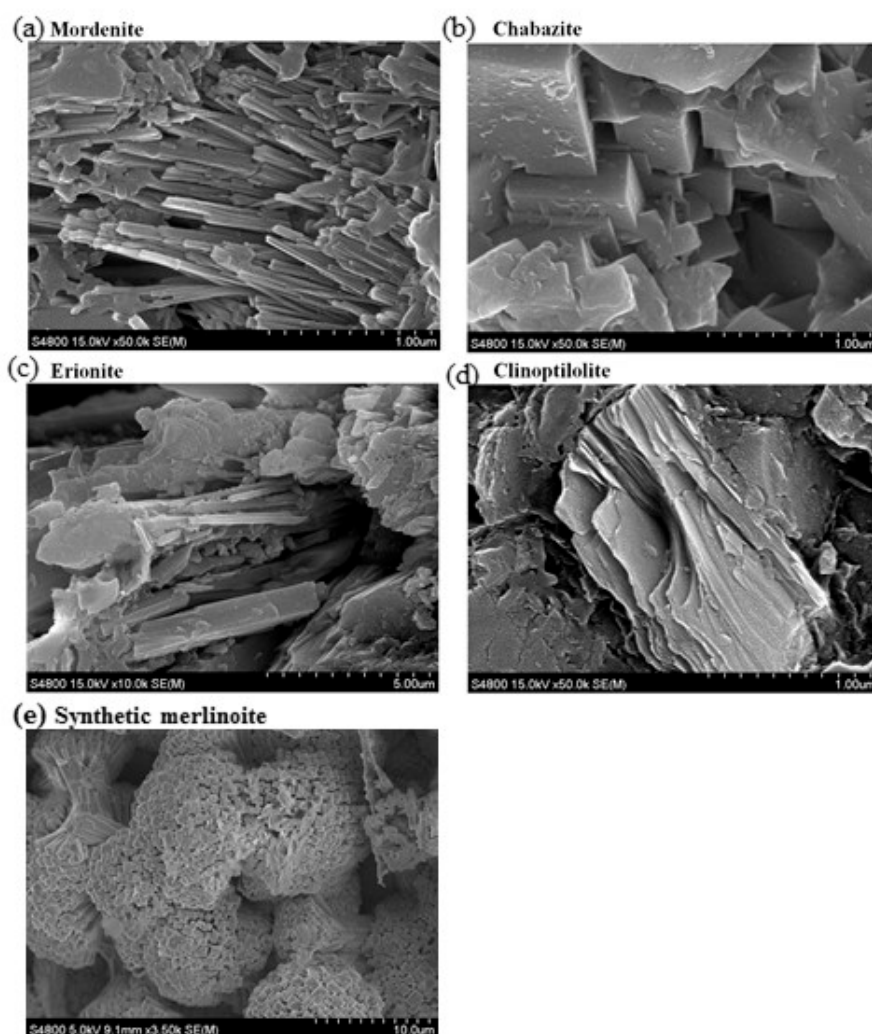

Figure 2. Morphology of the zeolites as found using Scanning Electron Microscopy. (**a**) Mordenite; (**b**) chabazite; (**c**) erionite; (**d**) clinoptilolite; and, (**e**) synthetic merlinoite.

Table 1. Weight percentages of the chemical composition of zeolites by EPMA (n: analytic grain numbers; Si/Al and 2Ca + Mg + Na + K based on 96 oxygen in molar ratio). Specific surface area was determined by the BET method.

Zeolite	n	SiO_2	Al_2O_3	MgO	CaO	Na_2O	K_2O	Total (wt %)	Formula	Si/Al	2Ca + 2Mg + Na + K	Specific Surface Area (m^2/g)
Mordenite	26	71.36	10.58	0.04	3.33	1.12	1.98	88.42	$(Ca_{2.05}, Mg_{0.03}, Na_{1.24}, K_{1.45})Al_{7.14}Si_{40.93}O_{96}$	5.73	6.8	85.1468
Chabazite	5	54.51	14.98	1.27	2.23	3.41	3.42	79.95	$(Ca_{1.58}, Mg_{1.26}, Na_{4.36}, K_{2.89})Al_{11.65}Si_{36.03}O_{96}$	3.09	12.9	378.5544
Erionite	4	61.45	14.38	1.04	3.57	0.52	4.40	85.37	$(Ca_{2.34}, Mg_{0.95}, Na_{0.62}, K_{3.44})Al_{10.35}Si_{37.58}O_{96}$	3.63	10.6	395.2574
Clinoptilolite	14	69.14	12.82	0.05	3.70	1.58	1.94	89.38	$(Ca_{2.27}, Mg_{0.04}, Na_{1.75}, K_{1.42})Al_{8.63}Si_{39.58}O_{96}$	4.58	7.7	22.0504
Merlinoite	13	52.15	20.19	0.04	0.42	2.61	13.07	88.53	$(Ca_{0.29}, Mg_{0.04}, Na_{3.21}, K_{10.59})Al_{15.07}Si_{33.09}O_{96}$	2.19	13.8	3.4623

3. Experimental Methods

In order to understand the ion exchange and adsorption proportions of zeolites, we first removed excess impurities in the zeolites. The zeolites were washed in pure water and were ultrasonically cleaned three times to remove salts and excess adsorbed cations, since many of our zeolite samples were collected from natural saline lakes [19]. The zeolites were then oven-dried at 110 °C for 24 h. The samples were then ground to powder and sieved through an 80 mesh sieve. A standard solution of 1000 mg/kg NH_4^+ (Merck Chemistry, NH_4Cl) was diluted for our experiment. A quantity of 5 g of zeolite powder was added to 500 mL of NH_4^+ solution (solid/liquid = 1/100). A blank experiment was conducted in correlation with the above experiments. Zeolites were immersed individually in different ammonium concentrations of 20, 50, and 100 mg/kg, and the temperature was held at 30 °C. In the temperature-controlled experiments, we only used mordenite, chabazite, and erionite in NH_4^+ solutions of 50 mg/kg at different temperatures (5, 15, 30, 40, and 50 °C). All of the experiments were carried out in a thermostatic water bath.

After commencing the experiments, 5 mL of solution (test samples) was removed from the container every 6 h over a seven-day time span to measure the cation concentrations. Each test sample was diluted to measure the concentrations of NH_4^+, Na^+, K^+, Ca^{2+}, and Mg^{2+}. Released cations Na^+, K^+, Ca^{2+}, and Mg^{2+} were determined using Inductively Coupled Plasma Atomic Emission Spectrometry (ICP-AES, Horiba Scientific, Ultima II type, Kyoto, Japan). Ammonium concentrations were measured using a UV–vis Spectrophotometer (Metretech Inc., SP 8001 type, Taipei, Taiwan) at a transparent wavelength of 640 ± 1 nm. The equilibrium concentration of each cation was collected within the seven-day-long experiment, and the final result was determined.

The specific surface area of each zeolite sample was measured using a Specific Surface Area and Pore Size Distribution Analyzer (SSA, Micromeritics, model ASAP2020, Merit Science Corporation, Norcross, GA, USA). The samples were pretreated in a vacuum environment at 393.15 K overnight to clean their surface and were then analyzed at 77 K (liquid nitrogen boiling temperature). The surface area value was determined by using the BET equation to fit the relative pressure curve that ranges from 0.06 to 0.2. The test results were calculated by averaging the values of the six measurements (Table 1). Moreover, we determined the grain size of treatment zeolites using a laser particle analyzer (Malven Masterizer 2000 type, Malven Analysitcal, Malven, UK), which is capable of detecting particle sizes from 0.02 to 2000 μm.

4. Results and Discussion

4.1. Percentage of Ion Exchange and Adsorption in Different Concentrations

As one cation invades a zeolite structure, it can be adsorbed on the external surface of the channels or exchanged with the original cation that occupies the zeolitic cages. According to the fundamentals

of ion exchange between solid and liquid phases [7,8], ion exchange between a zeolite frame and the aqueous ammonium solution can be expressed by the following Equation (1):

$$Z - M^{n+} + nNH_4^+ \leftrightarrow Z - nNH_4^+ + M^{n+} \tag{1}$$
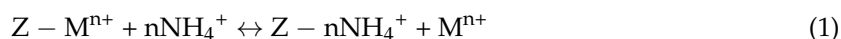
where Z and M represent the zeolite and bonding cations in the zeolite, respectively; and, n is the number of the electric charge. Accordingly, we assume that total ammonium removal ($NH_4^+{}_{total}$) from the solution equals the sum of ion exchange ($NH_4^+{}_{ion}$) and adsorption ($NH_4^+{}_{ads}$) of ammonium in zeolites, according to Equation (2), below:

$$NH_4^+{}_{ion} + NH_4^+{}_{ads} = NH_4^+{}_{total} \tag{2}$$

Based on Equation (1), we assume that the released cations are equal to the ion exchange capacity ($NH_4^+{}_{ion}$) [8,20], which can be determined by Equation (3). Finally, the adsorption capacity of zeolite can be derived from Equations (2) and (3). The adsorption capacity ($NH_4^+{}_{ads}$) is given by Equation (4):

$$NH_4^+{}_{ion} = [Na^+] + [K^+] + 2[Ca^{2+}] + 2[Mg^{2+}] \tag{3}$$

$$NH_4^+{}_{ads} = NH_4^+{}_{total} - NH_4^+{}_{ion} \tag{4}$$

As shown in Table 2, when we changed the ammonium concentration, we observed that the proportions of ion exchange and adsorption capacities for each zeolite were altered. In the 20 mg/kg ammonium solution, most zeolites have higher ion exchange capacities, and more than 90% of ammonium removal is dependent on the ion exchange mechanism. Only mordenite and erionite show lower than 70% ammonium removal by ion exchange. The results of Table 2 imply that a higher ammonium concentration leads to a higher proportion of adsorption by zeolites. The percentage of ion exchange capacity ranges between 64% and 99% at an initial concentration of 20 mg/kg, and it declines to 54–85% at a higher concentration of 50 mg/kg. In the highest ammonium concentration of 100 mg/kg, this percentage decreases to 52–70%. This phenomenon has also been proven in other studies [21]. Comparing the ammonium removal capacity of clinoptilolite between ours and that found by Liu et al. [8] under the same conditions for 100 mg/kg, we found that the total ammonium removal capacity for their clinoptilolite mixed with heulandite and quartz was approximately 0.3 meq/g and the ion exchange capacity was approximately 0.2 meq/g [8]; in this study, the total ammonium removal capacity of our zeolites is higher than 0.4 meq/g, and the ion exchange capacity is higher than 0.2 meq/g (Table 2).

Table 2. Results of zeolite removal of NH_4^+ and the proportions of ion exchange and adsorption in different initial NH_4^+ concentrations.

NH_4^+ Concentration	Zeolites	$NH_4^+{}_{ion}$ (meq/g)	Ion Exchange (%)	$NH_4^+{}_{ads}$ (meq/g)	Adsorption (%)	$NH_4^+{}_{total}$ (meq/g)
20 mg/kg	Mordenite	0.062	64%	0.034	36%	0.096
	Chabazite	0.103	97%	0.003	3%	0.106
	Erionite	0.073	68%	0.034	32%	0.108
	Clinoptilolite	0.087	90%	0.010	10%	0.097
	Merlinoite	0.091	99%	0.001	1%	0.092
50 mg/kg	Mordenite	0.128	54%	0.110	46%	0.238
	Chabazite	0.163	65%	0.088	35%	0.251
	Erionite	0.134	56%	0.104	44%	0.238
	Clinoptilolite	0.120	55%	0.097	45%	0.217
	Merlinoite	0.194	85%	0.034	15%	0.228
100 mg/kg	Mordenite	0.234	55%	0.189	45%	0.423
	Chabazite	0.277	59%	0.190	41%	0.467
	Erionite	0.238	52%	0.219	48%	0.457
	Clinoptilolite	0.240	58%	0.172	42%	0.412
	Merlinoite	0.277	70%	0.120	30%	0.398

4.2. The Relationship of Ion Exchange and Adsorption with Zeolite Composition

Each zeolite possesses a different structure and composition. Theoretically, the number of exchangeable cations in a zeolite will influence its ion exchange capacity, and the channel pore size of a zeolite will impact its adsorption capacity. The pore sizes and numbers of channels in zeolites are somewhat dependent on the Si/Al ratio [19]. Substitution of silicon by aluminum atoms in the crystal framework leads to additional negative charge, requiring balancing by IA and IIA cations (e.g., Na^+, K^+, Ca^{2+}, and Mg^{2+}) [19]. Therefore, we must compare the cation numbers and Si/Al ratios of zeolites with their ammonium removal ability.

Figure 3a presents the relationship between the ammonium ion exchange capacity and the Si/Al ratio of zeolites under initial NH_4^+ concentrations of 20, 50, and 100 mg/kg. The trend indicates that zeolites with lower Si/Al ratios (merlinoite, chabazite) have slightly higher ion exchange capacities ($NH_4^+_{ion}$). This may be somewhat influenced by the more exchangeable IA and IIA cations in zeolites with lower Si/Al ratio [16,17]. On the other hand, the adsorption capacity of a zeolite is primarily controlled by the zeolite structure. Therefore, we calculated the ammonium adsorption capacity and then compared it with the zeolite Si/Al ratio (Figure 3b). We discovered that zeolites with higher Si/Al ratios have slightly higher ammonium adsorption capacities ($NH_4^+_{ads}$), but that of erionite is especially higher. Leyva-Ramos et al. [10,22] compared the ion exchange capacities of chabazite and clinoptilolite and also reported that natural chabazite has a higher ion exchange capacity, which is similar to our result shown in Figure 3a.
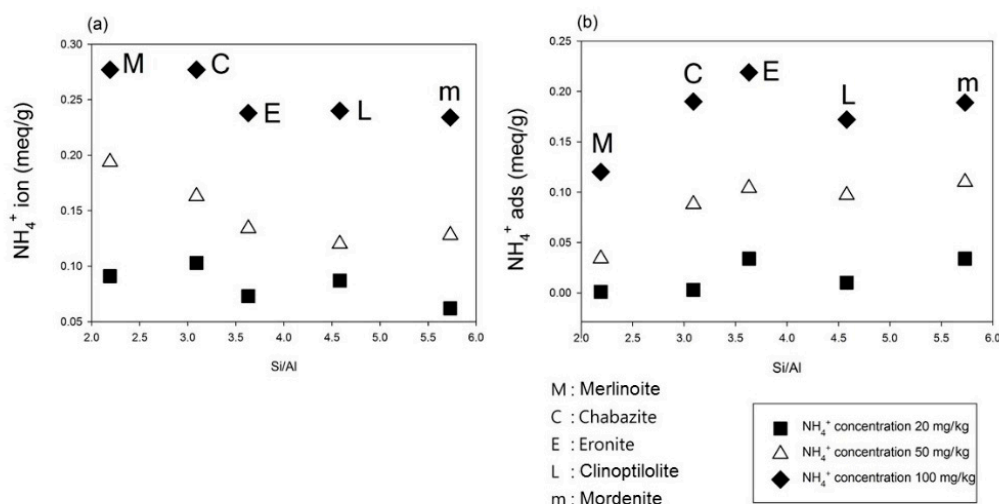

Figure 3. Relationships of (**a**) ion exchange and (**b**) adsorption capacities with the Si/Al ratios of zeolites for different ammonium solutions.

We then compared the adsorption capacity ($NH_4^+_{ads}$) and the ion exchange capacity ($NH_4^+_{ion}$) with the sum total of IA and IIA cations in zeolites. Mordenite, clinoptilolite, and erionite have lower ion exchange capacities due to their lower cation contents (Figure 4), while chabazite and synthetic merlinoite with higher cation contents have higher ion exchange capacities (Figure 5). The results indicate a positive correlation between the cation content and the ion exchange capacity in all concentrations (Figure 5).

Low Si/Al zeolites (merlinoite, chabazite, and erionite) have eight-ring channels and a smaller aperture size, but high Si/Al zeolites (clinoptilolite and mordenite) have eight-ring, 10-ring, and 12-ring channels and a larger aperture size. The adsorption capacity of zeolites is affected by the aperture size of channels because larger apertures facilitate the passing through of cations. Figure 3b shows that the higher Si/Al zeolites have slightly higher adsorption capacities than do the others. When we only consider the behavior of ion exchange, the diameter of NH_4^+ is approximately 2.96 Å [21], which passes through zeolite channels very easily. On the other hand, the diameter of a hydrated NH_4^+

ion is approximately 6.62 Å [19], which is larger than the aperture of most zeolites; thus, the hydrated ion cannot freely enter such small pores. Although the aperture size of a zeolite only reflects the average result of an ideal crystal, the specific surface area of zeolites may also affect the adsorption results.
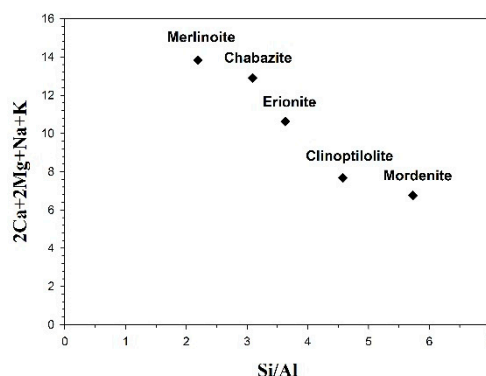

Figure 4. Relationship between the Si/Al ratio and IA and IIA cation content in zeolite compositions.
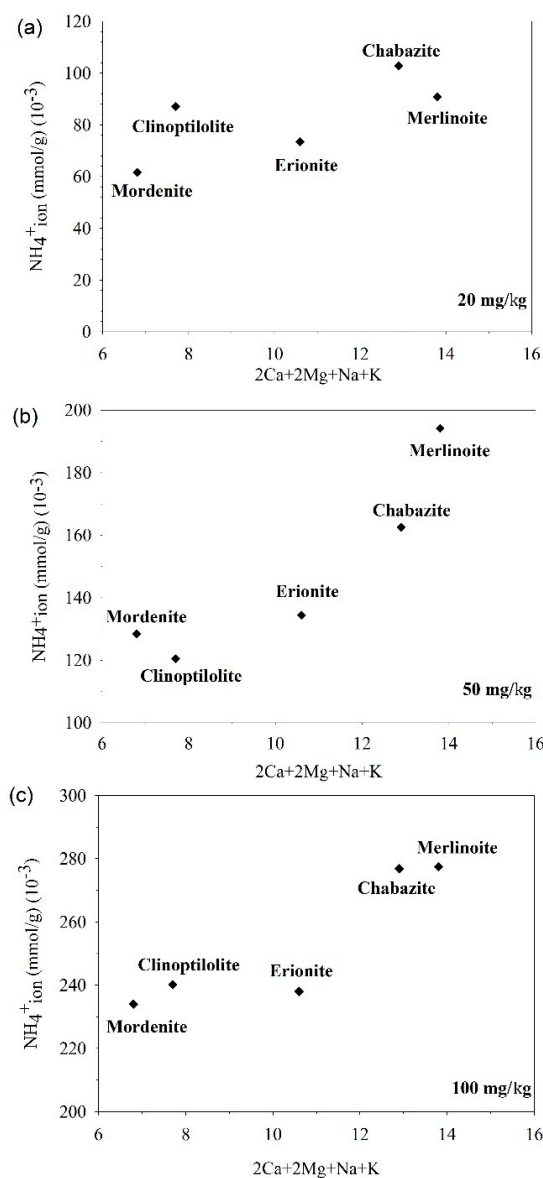

Figure 5. Relationship between IA and IIA cation content and ion exchange capacity in initial concentrations of (**a**) 20 mg/kg, (**b**) 50 mg/kg, and (**c**) 100 mg/kg.

4.3. Specific Surface Area of Zeolites

We attempted to measure the specific surface area (SSA) of zeolites in order to investigate its role in adsorption and ion exchange capacities. Erionite and chabazite have larger SSAs of 395.26 and 378.55 m^2/g, respectively (Table 1), while mordenite and clinoptilolite show SSAs of 85.15 and 22.05 m^2/g, respectively. Synthetic merlinite has an SSA of only 3.46 m^2/g, which constitutes the smallest SSA.

SSA reveals no relationship with ion exchange capacity in any concentration (Figure 6b,d,f). The SSA results from Figure 6a,c,e show that higher-SSA zeolites (i.e., erionite, chabazite, mordenite, and clinoptilolite) have higher adsorption capacity than synthetic merlinoite, especially at high concentrations of 50 mg/kg and 100 mg/kg (Figure 6c,e), with a nonlinear relationship. Up to 100 m^2/g, the adsorption capacity exhibits an obviously positive trend with the SSA. Interestingly, however, as the SSA rises above the critical value of 100 m^2/g, the adsorption capacity no longer increases. This implies that the adsorption capacity has become saturated.
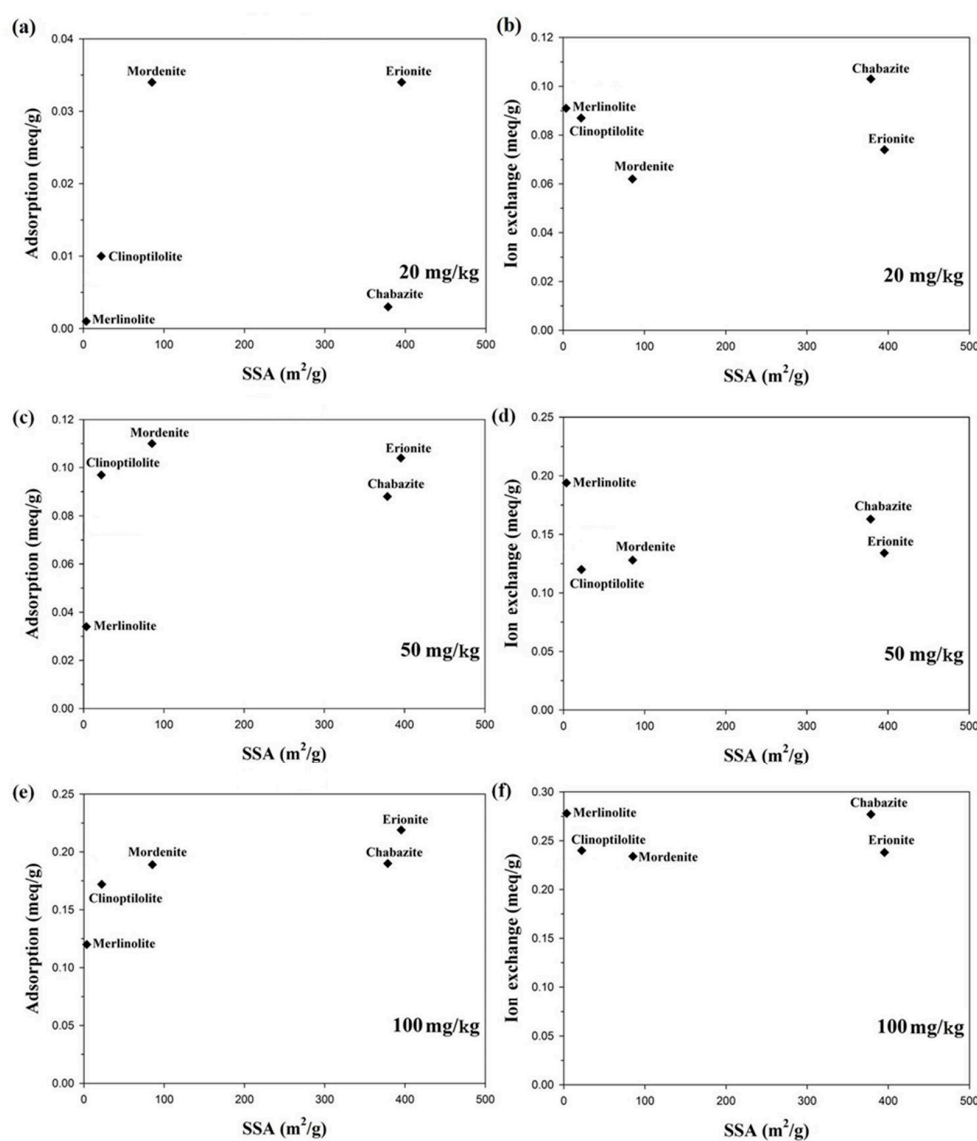

Figure 6. Relationship between specific surface area (SSA) and (**a**) adsorption capacity in a concentration of 20 mg/kg; (**b**) ion exchange capacity in a concentration of 20 mg/kg; (**c**) adsorption capacity in a concentration of 50 mg/kg; (**d**) ion exchange capacity in a concentration of 50 mg/ kg; (**e**) adsorption capacity in a concentration of 100 mg/kg; and, (**f**) ion exchange capacity in a concentration of 100 mg/kg.

4.4. Temperature Effect

4.4.1. Total Ammonium Removal at Different Temperatures

In order to examine the effect of temperature on zeolite ammonium removal, we selected three of the more effective ammonium-adsorbing zeolites (i.e., mordenite, chabazite, and erionite) to immerse in 50 mg/kg NH_4^+ solution at 5, 15, 30, 40, and 50 °C. We calculated the percentage of total NH_4^+ removal under these different temperatures (Figure 7). This experiment revealed that the percentage of NH_4^+ removal reaches its highest level at 30 °C for these zeolites. The percentages of NH_4^+ removal were 77.91% for mordenite, 81.96% for chabazite, and 75.94% for erionite at 30 °C. However, when the temperature is higher or lower than 30 °C, the ammonium removal ability decreases rapidly. This result agrees well with previous research [10,11,15,23–25], which also demonstrated that the highest ammonium removal efficiency occurs at room temperature (25–35 °C). At low temperatures of 5 and 15 °C, chabazite and erionite have better removal abilities than mordenite (Figure 7). It is very interesting that the ammonium removal ability of mordenite shows an extreme decrease as the temperature reaches values lower than 20 °C. We know the rate of ion exchange should decrease as the temperature drops and the adsorption ability should decrease as the temperature goes up.
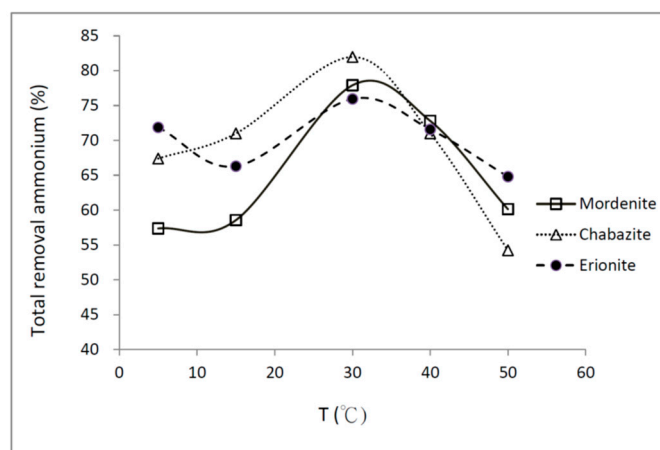

Figure 7. Percentage of total ammonium removal for zeolites at an initial NH_4^+ concentration of 50 mg/kg at different temperatures.

4.4.2. Zeolite Selectivity at Different Temperatures

In order to compare ion exchange mechanisms, it is necessary to understand the cation selectivity of zeolites. We calculated the content of cations in solution and in zeolites at equilibrium. The equilibrium constant K_i of element i follows Equation (5):

$$K_i = (C_i)z/(C_i)s \tag{5}$$

where $(C_i)s$ is the concentration of element i in the solution and $(C_i)z$ represents the concentration of element i in the zeolite. A high K_i value indicates that cations tend to be sorbed easier into the zeolite at equilibrium. Therefore, the reciprocal $1/K_i$ can be regarded as the cation release ability of element i from the zeolite. Table 3 presents each cation's release ability among the zeolites at different temperatures. Interestingly, our results demonstrate that the release ability $(1/K_i)$ of all elements changes with temperature. This implies that zeolite selectivity changes with temperature and zeolite type. Moreover, most conditions reveal that the ion release priority follows Na > Ca > K for mordenite, chabazite, and erionite; however, when the temperature approached 30–40 °C, the release ability of all elements rose, and the release ability of K increased markedly in mordenite and erionite. This result reveals that the ion exchange ability of zeolite reaches a maximum at 40 °C (Table 3). The irregular release of Mg may be due to the zeolite structure controlling the release sequence of Mg. Mordenite

possesses a lower Mg content than chabazite and erionite (Table 1), but the release ability of Mg in mordenite has higher priority than Mg in chabazite and erionite (Table 3). Although chabazite has higher potassium content (Table 1), its potassium was never released into the solution in our experiments (Table 3). This indicates that the zeolite type also influences the ion release ability.

Table 3. Release ability of each cation in zeolites and zeolite selectivity under different temperatures.

Mordenite	$1/K_{Mg}$	$1/K_{ca}$	$1/K_{Na}$	$1/K_K$	Release Priority	Zeolite Selectivity
5 °C	0.554	0.082	0.169	0	Mg > Na > Ca	Mg < Na < Ca < K
15 °C	0.768	0.055	0.112	0	Mg > Na > Ca	Mg < Na < Ca < K
30 °C	0.961	0.096	0.343	0.040	Mg > Na > Ca > K	Mg < Na < Ca < K
40 °C	1.256	0.100	0.344	0.111	Mg > Na > K > Ca	Mg < Na < K < Ca
50 °C	0.919	0.057	0.247	0	Mg > Na > Ca	Mg < Na < Ca < K
Chabazite	$1/K_{Mg}$	$1/K_{ca}$	$1/K_{Na}$	$1/K_K$		
5 °C	0	0.012	0.176	0	Na > Ca	Na < Ca < Mg = K
15 °C	0.008	0.005	1.951	0	Na > Mg > Ca	Na < Mg < Ca < K
30 °C	0.007	0.004	0.310	0	Na > Mg > Ca	Na < Mg < Ca < K
40 °C	0	0	0.133	0	Na	Na < Ca = Mg = K
50 °C	0	0	0.158	0	Na	Na < Ca = Mg = K
Erionite	$1/K_{Mg}$	$1/K_{ca}$	$1/K_{Na}$	$1/K_K$		
5 °C	0	0.019	8.339	0	Na > Ca	Na < Ca < K = Mg
15 °C	0	0.008	1.605	0	Na > Ca	Na< Ca < K = Mg
30 °C	0	0.008	1.915	0.006	Na > Ca > K	Na < Ca < K = Mg
40 °C	0	0.009	4.026	0.011	Na > K > Ca	Na < K < Ca = Mg
50 °C	0	0	1.028	0	Na	Na < Ca = K = Mg

Previous studies often use clinoptilolite to explore the ranking of cation selectivity [23,26,27]. Their results suggest the order K > Na > Ca > Mg. However, Lin et al. [8] found a different cation selectivity of clinoptilolite following the sequence Mg > K > Ca > Na. This result is congruent with our results. Our result also shows K > Ca > Na under most conditions, but the selectivity sequence of K and Ca changes at 40 °C for mordenite and erionite. This phenomenon gives us a hint that a higher temperature promotes the exchange of large cations with ammonium ion. Regular selectivity may directly reflect the ionic diameters of cations. The ionic diameter of K (2.66 Å) is larger than that of Ca (1.98 Å); that of Ca is larger than that of Na (1.9 Å); and, that of Na is larger than that of Mg (1.3 Å) [19]. This result indicates that efforts to determine the release ability of cations should consider the cation size and the effect of the positions within the cage.

4.5. Kinetic Diffusion of Ammonium

The kinetic diffusion of ammonium in zeolites is another crucial mechanism controlling the mass transport and should be considered in analysis. When mass transport occurs in the solid phase, we need to consider the time-varied diffusion coefficient. The diffusion rate is higher at the early stage but it decreases when approaching the equilibrium condition. In the case of 20 mg/g ammonium concentration, all zeolites reached equilibrium conditions after 100 h (Figure 8). Previous research defined the mass transport mechanisms for film diffusion (D_f) and effective particle diffusion (D_p) in a homogenous particle diffusion model [28,29]. The sorption on the spherical particles can be calculated through the effective particle diffusivity using Equation (6). As the rate of sorption is controlled by the liquid film diffusion, this rate can be expressed, as shown in Equation (7):

$$-\ln\left(1-\left(\frac{q_t}{q_e}\right)^2\right) = \frac{2\pi^2 D_P}{r^2}t \tag{6}$$

$$-\ln\left(1-\left(\frac{q_t}{q_e}\right)\right) = \frac{D_f C_s}{hr C_z}t \tag{7}$$

where q_t and q_e are the solute loadings on the adsorbent phase at time t and equilibrium (mg·g^{-1}), respectively; C_s (mg·L^{-1}) and C_z (mg·kg^{-1}) are the ion concentrations in solution and in the zeolite, respectively; r is the average radius of the zeolite particles obtained from our particle analysis (Table 4); t is the contact time (min); and h is the thickness of film around the zeolite particle (1×10^{-5} m for a poorly stirred solution) [30]. The coefficients of film diffusion (D_f) for all types of zeolites at different ammonium concentrations are significantly higher than those of particle diffusion (D_p) (Table 4). This result is consistent with previous works reporting ammonium sorption on natural zeolites at low initial ammonium concentrations [28–30] and it indicates that film diffusion should be the main mechanism controlling the mass transport. After comparing the diffusion data, we find that erionite has the maximal mass transport rate (Table 4).
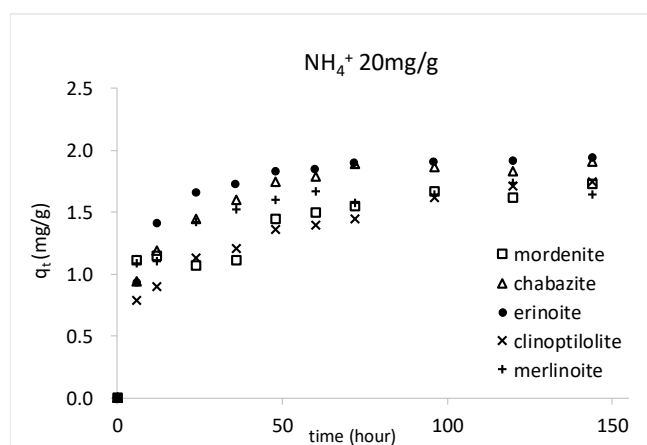

Figure 8. Evolution of ammonium sorption uptake versus time in 20 mg/g ammonium concentration at 30 °C.

Table 4. Diffusion parameters of zeolites in different ammonium concentrations at 30 °C.

Parameter	NH$_4^+$ Concentration	Mordenite	Chabazite	Erionite	Clinoptilolite	Merlinoite
Radius (μm)		8.7	14.0	16.3	10.7	17.9
Film diffusion D_f (μm^2·s^{-1})	20 mg/kg	0.3	2.1	4.9	0.3	1.1
	50 mg/kg	0.2	0.7	0.7	0.2	0.5
	100 mg/kg	0.2	0.5	0.4	0.2	0.2
Particle diffusion D_p (μm^2·s^{-1})	20 mg/kg	0.0016	0.0059	0.0097	0.0018	0.0139
	50 mg/kg	0.0013	0.0040	0.0068	0.0019	0.0079
	100 mg/kg	0.0014	0.0052	0.0052	0.0041	0.0053

5. Conclusions

In this study, we controlled several experimental factors, including the initial ammonium concentration, the zeolite composition, and the temperature. We also discussed the mechanisms governing ammonium removal by zeolites to study zeolite adsorption and ion exchange capacity. The results of applying various initial concentrations of NH$_4^+$ show that zeolites possess greater adsorption capacity under higher ammonium concentrations. In addition, it is found that ion exchange capacity is mainly controlled by the cation content in zeolites, while the adsorption capacity is mainly influenced by the Si/Al ratio and the SSA of zeolites. We discovered that mordenite has the highest adsorption capacity due to its sufficient SSA of nearly 100 m^2/g and due to having the largest Si/Al ratio. On the other hand, synthetic merlinoite possesses the lowest Si/Al ratio and the highest 2Ca + 2Mg + Na + K content, and it is also accompanied by a higher ion exchange capacity. Moreover, when we performed removal experiments at 5, 15, 30, 40, and 50 °C, we found that 30 °C most benefits ammonium adsorption among all zeolites. Furthermore, the cation selectivity of mordenite,

chabazite, and erionite follows the sequence of K > Ca > Na. This phenomenon involves the diameters of cations. The release of Mg is primarily controlled by the zeolite structure, and there is no specific trend among different zeolites. Finally, it was found that temperature changes the ion exchange ability of all zeolites and it slightly affects the release sequence of cations. The ammonium adsorption is mainly controlled by film diffusion, and the mass transportation rate of erionite is higher than those of the other zeolites examined.

Author Contributions: H.-F.C. coordinated and wrote this paper; H.-F.C. conceived the present idea and planned the experiments; Y.-J.L. and B.-H.C. conducted the experiments; I.Y. contributed EPMA analysis; S.Y.-H.L. analyzed the BET data of zeolites; R.-T.H. took part in producing the SEM images.

Conflicts of Interest: The authors declare no conflict of interest.

References

1. Kithome, M.; Paul, J.W.; Lavkulich, L.M.; Bomke, A.A. Kinetics of ammonium adsorption and desorption by natural zeolite clinoptilolite. *Soil Sci. Soc. Am. J.* **1998**, *62*, 622–629. [CrossRef]
2. Wiesmann, U. Biological nitrogen removal from wastewater. *Adv. Biochem. Eng. Biotechnol.* **1994**, *51*, 114–153.
3. Nguyen, M.L.; Tanner, C.C. Ammonium removal from wastewaters using natural New Zealand zeolites. *N. Z. J. Agric. Res.* **1998**, *41*, 427–446. [CrossRef]
4. Townsend, R.P.; Loizidou, M. Ion-exchange properties of natural clinoptilolite, ferrierite and mordenite: 1. Sodium-ammonium equilibria. *Zeolites* **1984**, *4*, 191–195. [CrossRef]
5. Mondale, K.D.; Carland, R.M.; Aplan, F.F. The comparative ion exchange capacities of natural sedimentary and synthetic zeolites. *Miner. Eng.* **1995**, *8*, 535–548. [CrossRef]
6. Green, M.; Mels, A.; Lahav, O.; Tarre, S. Biological ion exchange process for ammonium removal from secondary effluent. *Water Sci. Technol.* **1996**, *34*, 449–458. [CrossRef]
7. Ioannidis, S.; Anderko, A. Equilibrium modeling of combined ion-exchange and molecular adsorption phenomena. *Ind. Eng. Chem. Res.* **2001**, *40*, 714–720. [CrossRef]
8. Lin, L.; Lei, Z.; Wang, L.; Liu, X.; Zhang, Y.; Wan, C.; Lee, D.J.; Tay, J.H. Adsorption mechanisms of high-levels of ammonium onto natural and NaCl-modified zeolites. *Sep. Purif. Technol.* **2013**, *103*, 15–20. [CrossRef]
9. Weatherley, L.R.; Miladinovic, N.D. Comparison of the ion exchange uptake of ammonium ion onto New Zealand clinoptilolite and mordenite. *Water Res.* **2004**, *38*, 4305–4312. [CrossRef] [PubMed]
10. Leyva-Ramos, R.; Monsivais-Rocha, J.E.; Aragon-Piňa, A.; Berber-Mendoza, M.S.; Guerrero-Coronado, R.M.; Alonso-Davila, P. Removal of ammonium from aqueous solution by ion exchange on natural and modified chabazite. *J. Environ. Manag.* **2010**, *91*, 2662–2668. [CrossRef] [PubMed]
11. Alshameri, A.; Yan, C.; Al-Ani, Y.; Dawood, A.S.; Ibrahim, A.; Zhou, C.; Wang, H. An investigation into the adsorption removal of ammonium by salt activated Chinese (Hulaodu) natural zeolite: Kinetics, isotherms, and thermodynamics. *J. Taiwan Inst. Chem. Eng.* **2014**, *45*, 554–564. [CrossRef]
12. Englert, A.H.; Rubio, J. Characterization and environmental application of a Chilean natural zeolite. *Int. J. Miner. Process.* **2005**, *75*, 21–29. [CrossRef]
13. Widiastuti, N.; Wu, H.; Ang, H.M.; Zhang, D. Removal of ammonium from greywater using natural zeolite. *Desalination* **2011**, *277*, 15–23. [CrossRef]
14. Franus, W.; Wdowin, M. Removal of ammonium ions by selected natural and synthetic zeolites. *Gospodarka Surowcami Mineralnymi—Miner. Res. Manag*. **2010**, *26*, 133–148.
15. Alshameri, A.; Ibrahim, A.; Assabri, A.; Lei, X.; Wang, H.; Yan, C. The investigation into the ammonium removal performance of Yemeni natural zeolite: Modification, ion exchange mechanism, and thermodynamics (Clinoptilolite and montmorillonite). *J. Chem. Technol. Biotechnol.* **2016**, *91*, 1737–1746. [CrossRef]
16. Chen, H.F.; Fang, J.N.; Lo, H.J.; Song, S.R.; Chen, Y.L.; Chung, S.H.; Lee, C.Y.; Li, L.J.; Lin, I.C. The synthesis of merlinoite. *West. Pac. Earth Sci.* **2002**, *2*, 371–386.

17. Chen, H.F.; Lo, H.J.; Song, S.R.; Fang, J.N.; Chen, Y.L.; Li, L.J.; Lin, I.C.; Chung, S.H.; Lee, Y.T. The synthesis of phillipsite. *West. Pac. Earth Sci.* **2002**, *2*, 409–420.

18. Campbell, L.S.; Charnock, J.; Dyer, A.; Hilliber, S.; Chernery, S.; Stoppa, F.; Henderson, C.M.B.; Walcott, R.; Rumsey, M. Determination of zeolite-group mineral compositions by electron probe microanalysis. *Mineral. Mag.* **2016**, *80*, 781–807. [CrossRef]

19. Bish, D.L.; Ming, D.W. Natural zeolites: Occurrence, properties, applications. *Rev. Mineral. Geochem.* **2001**, *45*, 654.

20. Inglezakis, V.J. The concept of "capacity" in zeolite ion-exchange systems. *J. Colloid Interface Sci.* **2005**, *281*, 68–79. [CrossRef] [PubMed]

21. Zhu, Y.; Lee, Y. The study of removal ammonium by modified micro-pore zeolite ball. *Water Purif. Technol.* **2005**, *24*, 14–17. (In Chinese)

22. Leyva-Ramos, R.; Aguilar-Armenta, G.; Gonzalez-Gutierrez, L.V.; Guerrero-Coronado, R.M.; Mendoza-Barron, J. Ammonia exchange on clinoptilolite from mineral deposits located in Mexico. *J. Chem. Technol. Biotechnol.* **2004**, *79*, 651–657. [CrossRef]

23. Lebedynets, M.; Sprynsky, M.; Sakhnyuk, I.; Zbytniewski, R.; Golembiewski, R.; Buszewski, B. Adsorption of NH_4^+ ions onto a natural zeolite: Transcarpathian clinoptilolite. *Adsorpt. Sci. Technol.* **2004**, *22*, 731–741. [CrossRef]

24. Karadag, D.; Koc, Y.; Turan, M.; Armagan, B. Removal of ammonium ion from aqueous solution using natural Turkish clinoptilolite. *J. Hazard. Mater. B* **2006**, *136*, 604–609. [CrossRef] [PubMed]

25. Zheng, H.; Han, L.; Ma, H.; Zheng, Y.; Zhang, H.; Liu, D.; Liang, S. Adsorption characteristics of ammonium ion by zeolite 13X. *J. Hazard. Mater.* **2008**, *158*, 577–584. [CrossRef] [PubMed]

26. Sarioglu, M. Removal of ammonium from municipal wastewater using natural Turkish (Dogantepe) zeolite. *Sep. Purif. Technol.* **2005**, *41*, 1–11. [CrossRef]

27. Wang, Y.F.; Lin, F.; Pang, W.Q. Ammonium exchange in aqueous solution using Chinese natural clinoptilolite and modified zeolite. *J. Hazard. Mater.* **2007**, *142*, 160–164. [CrossRef] [PubMed]

28. Helfferich, F.G. *Ion Exchange*; McGraw-Hill: New York, NY, USA, 1962.

29. Valderrama, C.; Barios, J.I.; Caetano, M.; Farran, A.; Cortina, J.L. Kinetic evaluation of phenol/aniline mixtures adsorption from aqueous solutions onto activated carbon and hyper cross linked polymeric resin (MN200). *React. Funct. Polym.* **2010**, *70*, 142–150. [CrossRef]

30. Guaya, D.; Valderrama, C.; Farrana, A.; Luis Cortina, J. Modification of a natural zeolite with Fe(III) for simultaneous phosphate and ammonium removal from aqueous solutions. *J. Chem. Technol. Biotechnol.* **2016**, *91*, 1737–1746. [CrossRef]